Cellular Signalling 26 (2014) 2633–2644

Contents lists available at ScienceDirect

Cellular Signalling

journal homepage: www.elsevier.com/locate/cellsig

cGMP-dependent protein kinase I gamma encodes a nuclear localization signal that regulates nuclear compartmentation and function

Jingsi Chen [a,b,1], Jesse D. Roberts Jr. [a,b,c,d,*]

[a] Cardiovascular Research Center, Massachusetts General Hospital, Boston, MA, USA
[b] Harvard Medical School, Cambridge, MA, USA
[c] Departments of Anesthesia, Pediatrics, Massachusetts General Hospital, Boston, MA, USA
[d] Department of Medicine, Massachusetts General Hospital, Boston, MA, USA

ARTICLE INFO

Article history:
Received 10 July 2014
Accepted 15 August 2014
Available online 27 August 2014

Keywords:
cGMP-dependent protein kinase
cGMP signal transduction
Nuclear translocation
Smooth muscle cell

ABSTRACT

cGMP-dependent protein kinase I (PKGI) plays an important role in regulating how cGMP specifies vascular smooth muscle cell (SMC) phenotype. Although studies indicate that PKGI nuclear localization controls how cGMP regulates gene expression in SMC, information about the mechanisms that regulate PKGI nuclear compartmentation and its role in directly regulating cell phenotype is limited. Here we characterize a nuclear localization signal sequence (NLS) in PKGIγ, a proteolytically cleaved PKGI kinase fragment that translocates to the nucleus of SMC. Immuno-localization studies using cells expressing native and NLS-mutant PKGIγ, and treated with a small molecule nuclear transport inhibitor, indicated that PKGIγ encodes a constitutively active NLS that requires importin α and β for regulation of its compartmentation. Moreover, studies utilizing a genetically encoded nuclear phospho-CREB biosensor probe and fluorescence lifetime imaging microscopy demonstrated that this NLS controls PKGIγ nuclear function. In addition, although cytosolic PKGIγ-activity was observed to stimulate MAPK/ERK-mediated nuclear CREB signaling in SMC, NLS-mediated PKGIγ nuclear activity alone was determined to increase the expression of differentiation marker proteins in these cells. These results indicate that NLS-mediated nuclear PKGIγ localization plays an important role in how PKGI regulates vascular SMC phenotype.

1. Introduction

cGMP-dependent protein kinase I (PKGI) is a cGMP-stimulated phosphokinase that regulates SMC contractility [1–3]. This protein has an NH_2-terminal coiled-coil leucine zipper (LZ)-like autoinhibitory domain, tandem cGMP-binding pockets, and a catalytic region, which contains Mg^{2+}/ATP-binding, phosphokinase, and substrate recognition domains. Although PKGI is the product of one gene, alternate splicing of *PKGI* mRNA shuffles the 5′ exons and results in the protein expression of two PKGI isoforms, PKGIα and PKGIβ [4]. The variant LZ domains direct PKGI isoform homodimerization [5] and differential interactions with cytosolic anchoring proteins [6–8] and cytosolic compartmentation [7,9–12]. The PKGI isoform LZ domains also encode autoinhibitory (AI) domains that interact with the substrate recognition domain in the catalytic region and inhibit PKGI kinase activity in the absence of cGMP stimulation [13]. The PKGI isoforms exhibit differential cell and tissue expression [14]. Moreover, the PKGI expression is regulated through a number of mechanisms including cytokine-mediated signaling [15–17]. In SMC, cGMP-stimulated PKGI regulates the cytoskeleton by phosphorylating cytosolic protein targets that control intracellular Ca^{2+} levels, Ca^{2+}-sensitivity of contractile proteins, and perhaps the thin filament (reviewed in [18]).

PKGI also plays an important role in regulating cell phenotype [1,2]. PKGI has been detected in the nucleus of several cell types [12,19,20] and studies suggest that this compartmentation controls how PKGI influences gene expression. For example, over-expression of PKGIβ in PKGI-deficient baby hamster kidney (BHK) cells increases nuclear PKGI immuno-localization, the activation of *fos* promoter, through the activation of the cAMP response element, the AP-1 binding site, and the serum response element, and the induction of c-*fos* mRNA expression [20,21]. Also in these cells, PKGI transduces gene expression independently of PKA, calmodulin-dependent protein kinase, and MAPK signaling [22]. In SMC, PKGI increases the expression of contractile proteins, such as calponin and smooth muscle myosin heavy chain (MHC) [1,23–25], and decreases cell proliferation [26]. However, the mechanisms that regulate nuclear PKGI translocation are variable and incompletely understood. For example, in some experiments it is noted that PKGI does not localize to the nucleus or regulate gene expression [9,27–29]. In addition, the specific function of nuclear PKGI translocation

Abbreviations: PKGI, cGMP-dependent protein kinase I; NLS, nuclear localization signal; CREB, cAMP response element-binding protein.

* Corresponding author at: Cardiovascular Research Center, Massachusetts General Hospital, East, 149 13th St., Charlestown, MA 02129, USA. Tel.: +1 617 724 3104; fax: +1 617 726 5806.
E-mail address: roberts@cvrc.mgh.harvard.edu (J.D. Roberts).
[1] Current address: Department of Fetal Medicine, Obstetrics, and Gynecology, Third Affiliated Hospital of Guangzhou Medical University, Guangzhou, Guangdong, People's Republic of China.

http://dx.doi.org/10.1016/j.cellsig.2014.08.004
0898-6568/

in regulating SMC differentiation is incompletely understood. In some cells, PKGI regulates cytoplasmic signaling systems [30,31] that can transduce gene expression. These observations make it difficult to know whether PKGI nuclear localization alone controls gene expression. Understanding the mechanisms that regulate nuclear PKGI translocation and function will provide important information about how cGMP signaling regulates SMC phenotype.

Emerging evidence suggests that PKGI post-translational modifications control the nuclear PKGI localization and regulation of gene expression in SMC [32]. In these studies, PKGI cleavage in a hinge region of the molecule, which resides in a β-sheet that projects into the extramolecular milieu [33], was determined to generate an NH_2-terminal fragment of PKGI that remains in the perinuclear space and a constitutively active COOH-terminal fragment that contains the kinase domain, PKGIγ, that localizes to the nucleus [32]. The PKGI cleavage and nuclear PKGIγ localization was stimulated by cGMP and mechanisms that increase PKGI expression. Importantly, PKGI proteolysis was determined to be required for nuclear PKGI localization and activity. This is because PKGI cleavage, nuclear immunoreactivity, and transactivation of gene expression were decreased in cells expressing PKGI with mutations in the proteolytic site. Moreover, proprotein convertases (PCs) appear to play a part in regulating PKGI proteolysis and nuclear localization of PKGIγ [34]. This is because PKGI proteolysis was observed to be increased in a variety of cells in which select PCs are overexpressed and decreased in cells in which PC activity is defective or inhibited. Moreover, PC inhibition using membrane-permeable peptide decoys was determined to inhibit proteolysis-dependent PKGI nuclear localization in SMC. However, the mechanisms that govern PKGIγ nuclear localization and function are largely unknown.

Here we examined the mechanisms that regulate PKGIγ nuclear compartmentation and function in cells. Using cells expressing native and mutant PKGIγ, an inhibitor of importin α and β function, and immuno-localization studies, we report that PKGIγ harbors a classical NLS that regulates its nuclear localization. Moreover, employing a nucleus-localizing phospho-CREB biosensor and fluorescence lifetime imaging microscopy (FLIM), we determined that nuclear PKGIγ localization is required for the activation of CREB signaling. Of importance, in studies conducted with a MEK1/2 inhibitor, we observed that nuclear CREB activation by PKGIγ in SMC, but not in BHK cells, is also mediated through MAPK/ERK signaling. Lastly, by assessing the expression levels of SMC contractile proteins in transfected SMC using flow cytometry, we determined that nuclear but not cytoplasmic PKGIγ regulates the expression of cytoskeletal proteins that are indicative of SMC differentiation. Therefore, this work details mechanisms that regulate nuclear PKGI compartmentation and further enhances the view that the nuclear transport of PKGI has an important role in regulating SMC.

2. Materials and methods

2.1. Plasmid constructs and materials

The plasmids encoding NLS-ICAP and NLS-ICAP-ΔS^{133} were a kind gift of Michael Friedrich [35], and NH_2-terminal FLAG-epitope tagged vasodilator-stimulated phosphoprotein (FLAG-VASP) was from Michael Uhler [28]. pcDNA3-CFP was obtained from Addgene and pAcGFP1-Nuc, which encodes GFP-NLS, was purchased from Clontech. To generate pcDNA3-FLAG-PKGIγ, PCR was used to amplify a cDNA that encodes PKGIγ from pcDNA3-PKGIβ [32] with *BamH*I and *Xba*I restriction site ends. This fragment was then ligated in a 3′-position relative to a DNA fragment that specifies the FLAG epitope tag into pcDNA3. The PKGIγ cDNA fragment encodes a COOH-terminal portion of PKGIβ commencing with E^{168}. This is because amino acid microsequencing of immunopurified A7R5 SMC nuclear PKGIγ suggested that PKGIγ is generated by PKGI cleavage just NH_2-terminal to this amino acid [32]. Using this plasmid and site-directed mutagenesis, additional plasmids were constructed that encode PKGIγ with a mutant NLS (PKGIγ-ΔNLS) and PKGIγ that was predicted to lack kinase activity (PKGIγ-DK). The amino acid changes in the PKGIγ ΔNLS mutation are detailed below; the mutation in PKGIγ-DK corresponds to a T^{516}- > A switch in PKGIβ that was determined by Feil et al. to abolish PKGIβ phosphokinase activity [36]. The FLAG-PKGIγ and FLAG-PKGIγ-ΔNLS cDNA fragments were also introduced into the first open reading frame (ORF) of pCP2 (Clontech), a bicistronic plasmid with mCherry2 encoded in the second ORF following an internal ribosome entry site. The expression of the native and mutant PKGIγ transgenes was determined in soluble cell lysates as described previously [32]. The authenticity of the plasmid constructs was confirmed using dideoxynucleotide sequencing.

2.2. Cell culture and transfection

The fibroblast BHK cells and rat embryonal SMC A10 cells [37] were obtained from the American Tissue Culture Collection (ATCC). Rat aortic SMC (RAoSMC) were obtained using an explant method as previously described [26] and were used in the experiments before the seventh passage. The cells were maintained in DMEM containing 10% *v*/*v* FBS, penicillin (100 U/ml), and streptomycin (100 μg/ml) (Invitrogen) in a humidified 37 °C incubator with 5% CO_2. Cell transfection occurred using Lipofectamine 2000 (Invitrogen) or Xfect (Clontech) according to the manufacturer's instructions.

2.3. Cell imaging

To map PKGI immunoreactivity to the nucleus and cytosol of the cells, laser scanning confocal microscopy was performed using a microscope (Zeiss LSMS Pascal) with a pinhole and slide stage z-axis position set to obtain a ~2 μm-thick image in the mid-nuclear plane, as determined by the DAPI-image and described previously [32]. To test the effect of ivermectin on nuclear PKGIγ localization, cells were imaged using wide field microscopy (Nikon Eclipse Ti-E) and the mean fluorescence intensity in the nucleus and cytosol was determined using image analysis software (Nikon NIS-Elements). To determine the activation NLS-ICAP in fixed cells, time-correlated single-photon counting FLIM was performed using a Nikon TiE microscope equipped with a dedicated FLIM system (Becker & Hickl GmbH, Berlin Germany). The CFP donor fluorescence of the biosensor was excited with a 448-nm pulsed laser diode. The fluorescence signal from the cells was collected using a photomultiplier tube after the photons passed through a 40× oil immersion objective lens (NA 1.30) and a 460 nm wavelength long-pass filter. The data acquisition time adjusted so that $>5 \times 10^4$ photons were sampled per pixel. To demonstrate the co-expression of FLAG-PKGIγ transgenes and mCherry2, SMCs were transfected with the bicistronic plasmids, described above, fixed, permeabilized, and then exposed to anti-FLAG and Alexa 488-labeled secondary antibodies and then DAPI. The anti-FLAG, mCherry2, and DAPI fluorescence images were merged.

2.4. Detection of in vivo PKGI activity

After the cells were transfected with plasmids encoding PKGIγ constructs and FLAG-VASP, a cytosolic PKGI target, soluble proteins were collected in a reducing lysis buffer and resolved using SDS-PAGE. After electro-blotting the proteins onto a charged membrane, their FLAG transgene and phospho-VASP S^{239} immunoreactivity were detected as previously described [32].

2.5. Flow cytometry

Following transfection with plasmids, the SMCs were released from the plates using type IV collagenase, which we observed preserves membrane-bound mCherry2 fluorescence. Subsequently, the cells were fixed for 20 min in 2% paraformaldehyde in phosphate buffered saline, permeabilized with methanol, blocked with 5% bovine serum

albumin, and then reacted with fluorescently labeled anti-calponin, MHC, or equivalent amounts of isotype control antibodies. The anti-calponin antibody was purchased from Abcam (ab46794) and the anti-MHC antibody was obtained from Biomedical Technologies (BT-562, Stoughton MA USA). Subsequently, the cells were subjected to flow cytometry (LSRII, BD Biosciences) and at least 1×10^4 events were analyzed.

2.6. Data analysis

The lifetime images were analyzed by exponential function fitting and by determining goodness of fit of the photon decay curve using SPC Image software (Becker & Hickl GmbH). The CFP mean fluorescence lifetime (tm) was determined using a bi-exponential function model, as detailed in *Results*.

After the flow cytometry data was gated for dead cells and debris, and compensated for fluorescent spill-over, it underwent a linear-log transformation, as described by Klinke and Brundage [38] using custom scripts and a statistical programming language (R, [39]). The data were then gated based on the mCherry fluorescence to permit analysis of SMC contractile protein expression in cells that were transfected with the plasmids.

The experiments were repeated a minimum of three times and typical results are shown. The data are represented as mean ± S.D. and are compared using ANOVA. When indicated, a Tukey's range test was performed post hoc. Where indicated in the figures, $^*P \leq 0.05$.

3. Results

3.1. PKGIγ harbors an NLS that regulates PKGI nuclear compartmentation

A putative NLS was previously characterized in PKGIβ that appears to regulate its cGMP-dependent nuclear localization and gene expression transactivation [20]. This NLS consists of a single cluster of basic amino acids that resides within the catalytic region of PKGIβ (Fig. 1A). Some but not all mutations of the NLS were observed to inhibit cGMP-stimulated PKGI nuclear localization of PKGI. However, others determined that this NLS does not to fully regulate nuclear PKGIβ localization. Inspection of the amino acid sequence of PKGIγ reveals that this putative PKGIβ NLS is conserved within that kinase fragment (Fig. 1A). To test whether this NLS directs PKGIγ nuclear compartmentation, we used site-directed mutagenesis to make a single amino acid substitution of the P1 of the putative NLS of PKGIγ, as indicated in the figure. A similar approach was employed by Gudi et al. to characterize the function of the PKGIβ NLS [20]. As shown in Fig. 1B, transient transfection of BHK cells, which are cells that do not express appreciable levels of PKGI [20], with these constructs led to the expression of the PKGIγ transgenes of the expected size. To test the role of the putative NLS in regulating nuclear PKGIγ compartmentation, rat aortic SMC, A10 cells, and BHK cells were transiently transfected with these plasmids and one that we previously observed expressed PKGIβ with a COOH-terminal FLAG tag [32]. Subsequently, the PKGIγ transgenes were localized using indirect immunofluorescence and laser scanning confocal microscopy. As shown in Fig. 1C, whereas nuclear PKGI immunoreactivity was detected in the cells expressing PKGIγ and PKGIβ, it was not observed in those that were transfected with PKGIγ-ΔNLS. Moreover, it was noted that the nuclear PKGIγ compartmentation did not require cGMP stimulation, as was described for the full-length PKGI isoforms in other studies [32]. Although, we and others observed that PKGIβ overexpression increases nuclear PKGI immunoreactivity [8,11,32]. The specificity of the antibodies used to detect the FLAG epitope and the catalytic domain of PKGI is shown in Fig. 1D and elsewhere [32]. These data support the role of the NLS in regulating PKGIγ nuclear compartmentation.

3.2. PKGIγ nuclear localization is regulated through a classical NLS

Classical NLSs direct the nuclear importation of cytoplasmic cargo proteins through binding to the adapter protein importin α. Thereafter, NLS-bound importin α recruits importin β to the protein assembly, and importin β facilitates the binding of the trimeric complex to the nuclear pore complex and its transport into the nucleus [40,41]. Recently, ivermectin was observed to block importin α and β interaction and to inhibit the nuclear transport facilitated by prototypical NLS-mediated mechanism [42]. In order to test whether importin α and β play a role in regulating PKGIγ localization, BHK cells were transfected with plasmids that encode FLAG-PKGIγ and treated with and without ivermectin. Subsequently, the cells were fixed and permeabilized and the PKGIγ transgene was immunolocalized in the cells using an anti-FLAG antibody. To analyze the PKGIγ nuclear compartmentation the mean nuclear and cytoplasmic fluorescence ratios were quantified using a method described by others [42]. In control studies, the cells were transfected plasmids that encode FLAG-PKGIγ-ΔNLS or GFP-NLS, which is GFP that was engineered to have COOH-terminal tandem repeats of the SV40 large T-antigen NLS. As shown in Fig. 2, ivermectin exposure inhibited nuclear PKGIγ localization in the cells to levels detected for PKGIγ with the mutant NLS. Moreover, the disruption of NLS-mediated nuclear localization by ivermectin in these studies was confirmed by observing that it reduced the nuclear compartmentation of the GFP harboring a classical NLS. These studies indicate that the PKGIγ NLS requires importin α and β interaction to facilitate its nuclear localization in cells.

3.3. PKGIγ nuclear compartmentation regulates CREB activation in BHK cells

Although the studies detailed above characterized an NLS that regulates nuclear PKGIγ compartmentation, they do not demonstrate how it might control nuclear PKGI function. We and others have shown that nuclear PKGI localization is associated with transactivation of gene expression. However, even when detected in the nucleus, PKGIγ, the PKGI isoforms, and many of their targeted transcription factors also reside in the cytosol. Therefore, it would be important to understand whether the NLS-regulated PKGIγ nuclear compartmentation plays a direct role in controlling nuclear PKGI function. Because cGMP stimulates CREB-mediated signaling [43], and PKGIγ transactivates CREB signaling [32], we examined whether the PKGIγ NLS regulates nuclear CREB activation. Although CREB resides within the nucleus, it is detected and phosphorylated in the cytoplasm as well [44,45]. To improve the specificity of detecting CREB activation by PKGIγ residing in the nucleus, a phospho-CREB biosensor that is localized in the nucleus was employed for these studies. Previously, Friedrich et al. showed that a fusion protein consisting of the CREB kinase-inducible domain (KID), a linker, and the CREB-binding protein KID-interaction domain (KIX) sandwiched between an NLS and cyan fluorescent protein (CFP) on the NH_2-terminal end and yellow fluorescence protein (YFP) on the COOH-terminal (referred to as *NLS-ICAP*) exhibited reduced fluorescence resonance energy transfer (FRET) when PKA or calmodulin kinase induced CREB KID phosphorylation and KID-KIX interaction decreased CFP and YFP photonic interaction [35]). Because of the high variation in NLS-ICAP expression observed in the transfected cells during pilot studies, we first analyzed whether the activation of this phospho-CREB biosensor could be detected using fluorescence lifetime imaging microscopy (FLIM) instead of FRET. This is because in contrast with FRET, FLIM is insensitive to the expression level or concentration of the donor fluorescent protein.

Using fixed BHK cells expressing NLS-ICAP we defined the criteria to be used to model the photon decay curves of this probe and then tested whether FLIM could detect differences in the kinetics of the decay curves imparted by treatment with agents known to phosphorylate the CREB-based biosensor. As shown in Fig. 3A, the photon decay data

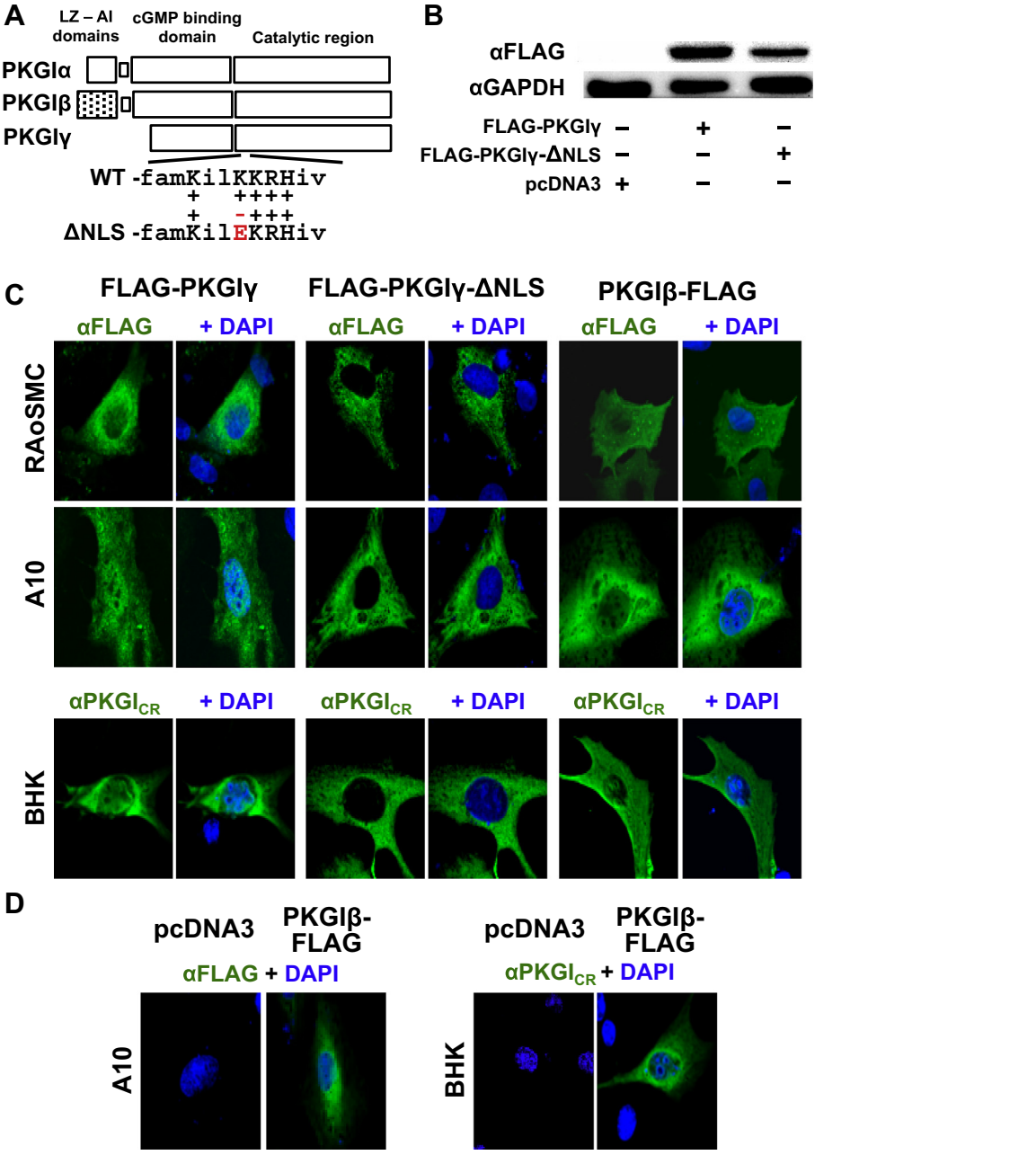

Fig. 1. PKGIγ encodes a NLS that directs its nuclear compartmentation. (A) The PKGIα/Iβ isoforms have linearly arranged variant leucine zipper (LZ)–autoinhibitory (AI) domains and a conserved cGMP-binding domain and a catalytic region, which is also common with the PKGIγ proteolytic fragment. The PKGI molecules also encode a putative NLS, which contains a cluster of positively charged amino acids (+), that is located as indicated. Plasmids were made that encode NH_2-terminal FLAG-tagged wild type (WT) PKGIγ and the indicated NLS K → E mutant (ΔNLS). (B) Lysates from BHK cells transfected with the FLAG-PKGIγ plasmid constructs exhibited expression of the transgenes by immunoblotting. After transfection with the plasmids encoding the indicated genes or pcDNA3, the cell lysates were resolved using SDS-PAGE, electroblotted on a charged membrane, exposed to the indicated antibodies, enzyme labeled secondary antibodies, and detected using chemiluminescence and a CCD camera system. (C) Although cells expressing PKGIγ and PKGIβ exhibited nuclear PKGI immunoreactivity, those expressing PKGIγ with a mutant NLS did not. The cells transfected with plasmids that encode the indicated PKGI transgenes were fixed, permeabilized, and interacted with the indicated antibodies that detect the FLAG epitope or catalytic region of PKGI (αPKGI$_{CR}$), and Alexa 488-conjugated secondary antibodies. Immunoreactivity was then assessed in a mid-nuclear optical slice obtained using laser scanning confocal microscopy. (D) The specificity of the antibodies used to detect the PKGI transgenes is shown here. The indicated cells were transfected with a plasmid that encodes PKGIβ·FLAG or pcDNA3, fixed, permeabilized, and then exposed to the indicated primary antibodies, Alexa 488-labeled secondary antibodies, DAPI, and assessed using laser scanning confocal microscopy.

of the CFP donor in NLS·ICAP can be modeled using the two-exponent equation as defined by others [46]. The goodness of fit of the modeling equation, particularly within the nuclear region, is shown in the Chi^2 image. Following sequential application of functions containing increasing numbers of exponential factors, the goodness of fit of the model is first optimal when a two exponent equation is applied. Moreover, inspection of the photon decay curve residual data shows that there is no systematic departure from the model following the application of a bi-exponential equation. These data are in agreement with those of others showing that CFP photon decay is efficiently modeled using a two-exponent equation [47]. Because cell fixation can affect the efficiency of protein fluorescence, we tested whether NLS-ICAP activation could be detected in formaldehyde-fixed cells using FLIM. In these studies, NLS-ICAP was modulated using forskolin because this had been shown to phosphorylate and modulate FRET of this CREB KID-based biosensor [35]. As shown in Fig. 3B, we observed that treating fixed BHK

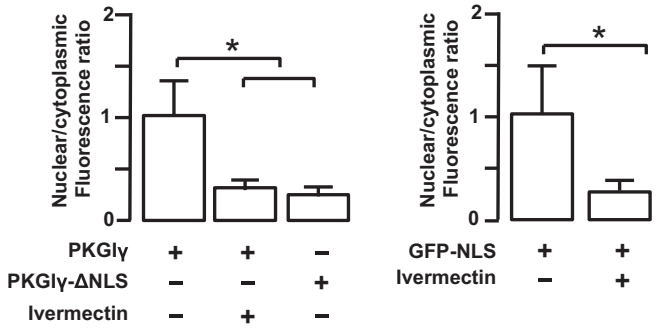

Fig. 2. Ivermectin inhibits nuclear PKGIγ localization. Rat aortic SMC were transfected with plasmids encoding the indicated PKGIγ constructs or GFP with three tandem repeats of the simian virus 40 large T-antigen NLS (GFP-NLS). After 1 h treatment with 25 μM ivermectin, or DMSO, and the cells were then fixed, permeabilized, and reacted with anti-$PKGI_{CR}$ and fluorescent secondary antibodies. Subsequently, wide-field fluorescence microscopy images were obtained and the ratio of nuclear-to-cytoplasmic fluorescence intensity was determined for a sample of cells whose images were obtained by an investigator masked with respect to the treatment group. The results were normalized to the mean value obtained from the DMSO-treated cells. $N = 10$ each group.

cells with forskolin decreased the CFP tm of NLS-ICAP. These studies indicate that FLIM can be used to detect NLS-ICAP activation in fixed BHK cells.

We next tested whether the PKGIγ NLS regulates nuclear PKGI phosphokinase activity through examining the activation of NLS-ICAP using FLIM. The anticipated model of the effect of PKGI-mediated NLS·ICAP phosphorylation on the CFP–YFP interaction is shown in Fig. 4A. The interaction between the photon donor CFP and acceptor YFP is expected to shorten the photon relaxation time in non-phosphorylated NLS·ICAP. In contrast, phosphorylation of the CREB KID is expected to increase phospho-KID and KIX interaction, decrease the CFP–YFP interaction, and prolong the photon relaxation time. For these studies, BHK cells were co-transfected with plasmids that encode NLS-ICAP and PKGIγ or PKGIγ-ΔNLS, fixed, and then the mean CFP photon relaxation time (tm) was determined following FLIM. The cellular compartmentation of the NLS·ICAP sensor is shown in Fig. 4B in typical BHK cells in the CFP fluorescence intensity image. The CFP intensity images confirmed the localization of NLS-ICAP within the nucleus of the cells. Moreover, the CFP tm heat map images demonstrate that this CREB KID-based biosensor is activated by PKGIγ primarily in the nucleus. Moreover, very little activation of NLS-ICAP is observed in the cytosol of the cells by PKGIγ and PKGIγ-ΔNLS. This supports the nuclear partitioning of this probe. The composite photon relaxation curve plot obtained from the cell nuclei and shown in Fig. 4C confirms a shift in the CFP photon release kinetics in the PKGIγ- but not the PKGIγ-ΔNLS-expressing BHK cells.

Next were defined the mechanisms through which nuclear PKGIγ regulates the phospho-CREB biosensor. In these studies, BHK cells were transfected with the indicated plasmids and either: 1) fixed and subjected to FLIM and the CFP tm was measured in the nuclear region, or 2) lysed and the indicated protein levels were detected using antibodies and protein blot hybridization. As shown in Fig. 5A, whereas PKGIγ increased the CFP tm of NLS-ICAP, PKGIγ-ΔNLS did not modulate the mean relaxation time of this phospho-CREB sensor. The data in Fig. 5B indicate that the lack of CFP tm modulation by PKGIγ-ΔNLS was not due to a deficiency in PKGIγ-ΔNLS kinase activity; PKGIγ-ΔNLS was observed to phosphorylate over-expressed VASP, a PKGI phosphorylation target and member of the Ena/VASP family of proteins that resides in the cytosol, and to cause a known shift in its apparent molecular weight when over-expressed in the BHK cells. Because the NLS·ICAP CREB KID harbors several amino acid residues that are targeted by kinases that phosphorylate CREB [35,48], we tested whether PKGIγ modulates the NLS-ICAP CFP tm through the consensus cyclic nucleotide-dependent phosphorylation site (-RRFS-, [49]). As shown in Fig. 5A, in contrast with the increase in CFP tm observed in the nuclei of BHK cells expressing PKGIγ and NLS·ICAP, those expressing PKGIγ and NLS·ICAP with a mutation in the KID residue mapping to CREB S^{133} did not exhibit a change in the photon relaxation time. Previous studies show that the control plasmid used in this experiment expresses NLS-ICAP ΔS^{133} and that the mutant NLS-ICAP is not phosphorylated by PKA [35].

To determine whether the activation of NLS-ICAP was due to the interaction of PKGIγ with another kinase, we tested whether NLS-ICAP CFP tm increased in cells that expressed an inactive PKGIγ kinase (PKGIγ-DK). Previous studies by Feil et al. demonstrated that mutation in an auto-phosphorylation site of PKGIα inhibited PKGI kinase activity [36]. Although it was unknown whether a corresponding mutation in PKGIγ would inhibit its activity, as shown in Fig. 6A, over-expressed PKGIγ-DK was observed to not phosphorylate FLAG-VASP in BHK cell lysates as determined by immunoblotting and exposure to phospho-VASP antibodies. In additional studies using anti-FLAG antibodies, we observed that BHK cells transfected with pcDNA3-FLAG-PKGIγ-DK expressed a protein of the expected size by immunoblotting and that the protein was observed within the nucleus by immunofluorescence microscopy (data not shown). Importantly, we found that BHK cells co-transfected with the plasmid that encodes PKGIγ-DK and NLS-ICAP did not exhibit the increase in CFP tm observed in the cells co-expressing PKGIγ (Fig. 6B).

Moreover, we tested whether the nuclear activation of NLS-ICAP by PKGIγ was mediated through PKA signaling. These studies were performed because under certain conditions, PKGI can cross-activate PKA signaling and because this biosensor was optimized to identify nuclear PKA activity. As shown in Fig. 7, the activation of NLS-ICAP by PKGIγ persisted during treatment of the BHK cells with myr-PKI, a membrane-permeable PKA inhibitor, even though this compound inhibited the forskolin-mediated increase in CFP tm. Together these studies indicate that the PKGIγ NLS regulates nuclear PKGI phosphokinase activity in BHK cells.

3.4. Nuclear and cytoplasmic PKGIγ regulate CREB activation in vascular SMC

Although the studies detailed in BHK cells above indicated that PKGIγ nuclear localization alone activates CREB, others observed in vascular SMC that PKGI can stimulate cytosolic MAPK signaling [30], which could indirectly regulate nuclear CREB signaling. To examine this possibility, we tested whether NLS-mediated PKGIγ nuclear localization alone regulates CREB activation in vascular SMC. For these studies, early passage rat aortic SMC were co-transfected with plasmids that encode NLS-ICAP and PKGIγ, with or without the NLS mutation detailed above, and the NLS·ICAP activation was assessed using FLIM after the cells were fixed. Pilot studies for this investigation confirmed that NLS-ICAP localizes to the nuclei of the SMC and that a bi-exponential model reliably details the photon relaxation curve of the CFP donor (data not shown).

Similar to the results in BHK cells, we observed that PKGIγ prolonged CFP tm in the aortic SMC (Fig. 8A). However, in contrast, PKGIγ-ΔNLS expression increased the CFP tm to a level that was intermediate between that determined in PKGIγ expressing and pcDNA3 transfected control SMC. To determine whether this change in NLS-ICAP activation was mediated through the cytoplasmic stimulation of MAPK signaling, aortic SMC were co-transfected with plasmids that encode NLS-ICAP and PKGIγ or PKGIγ-ΔNLS, and then treated with U0126, a MEK1/2 inhibitor, or DMSO, the diluent. As shown in Fig. 8B, U0126 treatment fully inhibited the PKGIγ-ΔNLS modulation of CREB activation. However, U0126 treatment only partially inhibited the change in CFP tm associated with PKGIγ expression. These data suggest that in SMC PKGIγ modulates CREB activation through direct nuclear mechanisms as well as cytosolic ones that require MAPK.

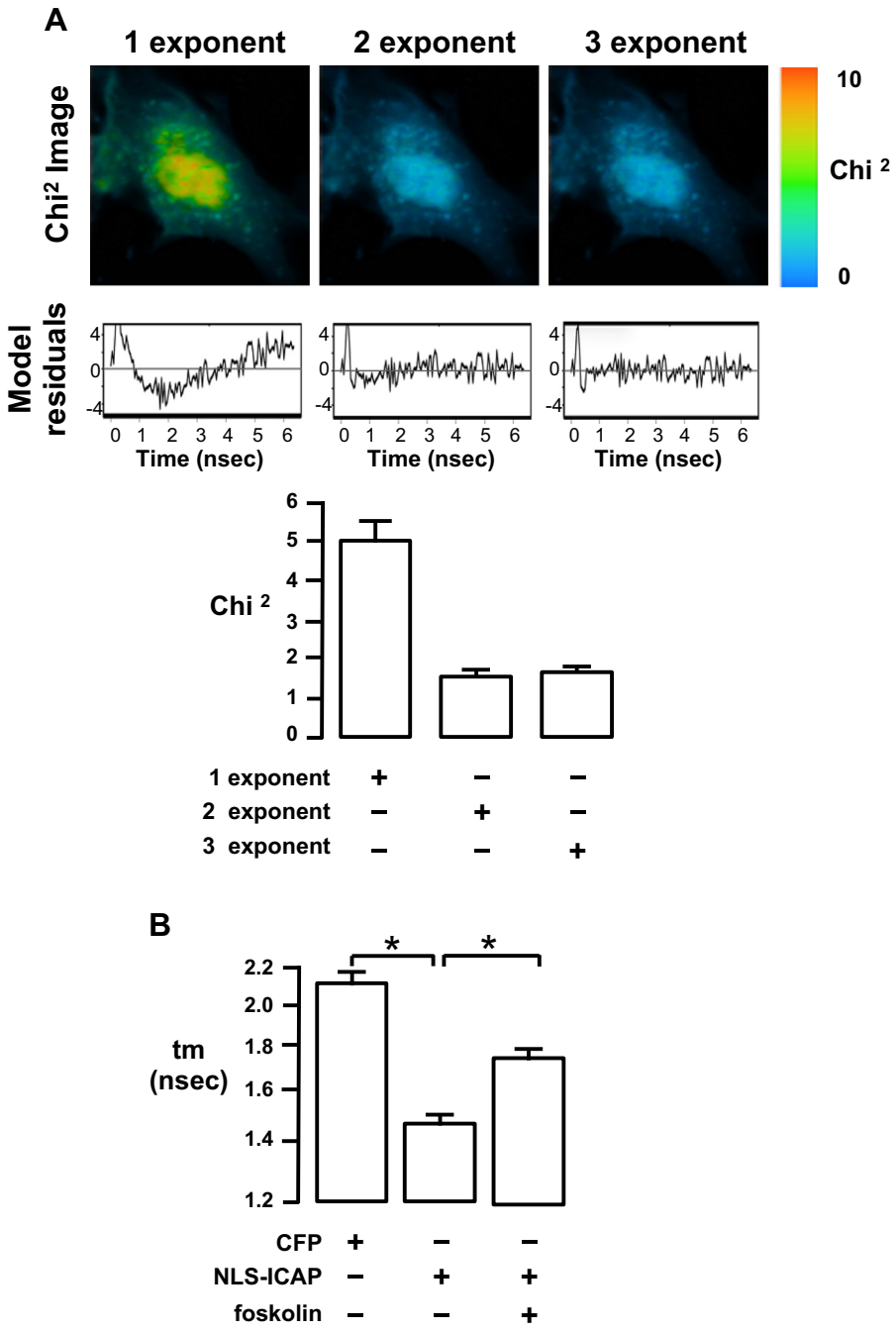

Fig. 3. Nuclear phospho-CREB biosensor fluorescence lifetime microscopy (FLIM) modeling. (A) BHK cells were transfected with a plasmid that encodes NLS-ICAP, a uni-molecular fluorescence resonance energy transfer (FRET)-based biosensor that localizes to the nucleus and is targeted by kinases that phosphorylate the CREB kinase-inducible domain (KID) (Friedrich 2010). NLS-ICAP phosphorylation increases CREB KID binding to the CBP KID-interaction domain (KIX) and thereby decreases the FRET of adjacent CFP and YFP molecules. After 40 h of serum starvation, the cells were fixed and then subjected to time-correlated single-photon counting FLIM. After step-wise application of a photon lifetime model equation with the indicated number of exponent time factors, representative Chi^2 images, model residuals, and Chi^2 data were obtained from a region of interest that included the whole cell. These data indicate that a two exponent model represents effectively the photon decay data as it results in a Chi^2 close to one without systematic variations in the model residuals. $N = 5$; $^*P \leq 0.05$. (B) One day after BHK cells were transfected with plasmids that encode CFP or NLS-ICAP, as indicated, and serum starved as described above, the cells were treated with 40 μM forskolin or DDW, fixed, and then subjected to FLIM and the mean photon decay times (tm) were determined using a two exponent photon decay model. Forskolin-treatment increases NLS-ICAP CFP tm similarly to the change in NLS-ICAP FRET reported previously [35]. $N = 10$ each group.

3.5. Nuclear PKGIγ regulates SMC differentiation

Previous studies indicate that cGMP regulates SMC differentiation through stimulating PKGI [1,43]. However, it is unknown whether PKGI can regulate SMC differentiation through nuclear mechanisms alone. Because the NLS detailed above was determined to regulate nuclear PKGIγ localization and activity, we next tested whether or not the PKGIγ compartmentation influences SMC differentiation. Primary vascular SMCs are difficult to transfect. To facilitate our studies, we employed plasmids and analytic techniques that would allow us to study PKGIγ-mediated changes of differentiation primarily in transfected SMC. We constructed bicistronic plasmids in which cDNA encoding PKGIγ or PKGIγ-ΔNLS was inserted into the first ORF while sequence encoding mCherry2, a red fluorescent protein that localizes to the plasma membrane [50], resided in the second ORF. Because of the relative efficiency of gene transcription, we observed that each SMC

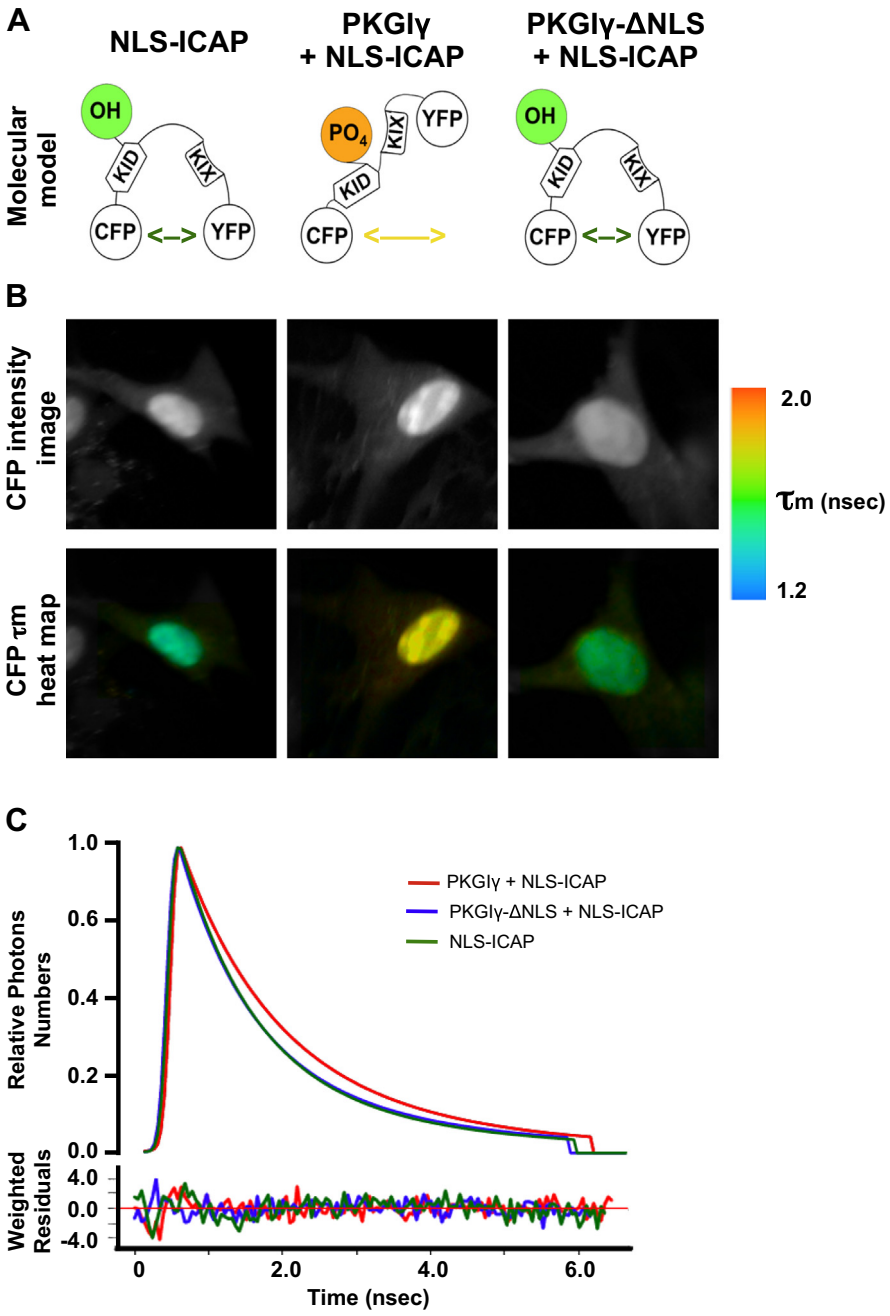

Fig. 4. Nuclear but not cytoplasmic PKGIγ regulates phospho-CREB biosensor activation. (A) BHK cells were transfected with plasmids that encode NLS-ICAP with or without those that encode the indicated PKGIγ constructs or pcDNA3. Shown are the anticipated molecular configurations of NLS-ICAP residing in the nucleus in the PKGIγ-expressing cells. Should PKGIγ phosphorylate nuclear NLS-ICAP then the CFP-YFP distance would increase as reflected by a greater tm. In contrast, should nuclear NLS-ICAP not be phosphorylated by PKGIγ-ΔNLS, then the tm would likely be unchanged and the CFP tm would be comparable with the one determined in the control cells. (B) Representative CFP fluorescence intensity images confirm that NLS-ICAP predominantly localizes to the nucleus of cells. The CFP tm heat map images show that PKGIγ but not PKGIγ-ΔNLS increases the NLS-ICAP CFP tm, particularly in the nuclear compartment, suggesting that PKGIγ but not PKGIγ-ΔNLS regulates nuclear CREB activation. (C) The photon decay curves in the BHK cells expressing the indicated transgenes confirm the modulation of NLS-ICAP CFP photon relaxation time by PKGIγ but not PKGIγ-ΔNLS. The distribution of the weighted residuals supports the validity of a bi-exponential decay curve employed here in modeling NLS-ICAP CFP tm.

transfected with this construct that exhibited mCherry2 fluorescence also expressed the PKGIγ transgene encoded by the first ORF (as shown in typical cells in Fig. 9A). Therefore, to examine the effect of PKGIγ nuclear compartmentation on SMC differentiation, we gated the flow cytometry fluorescence data to select for SMC that exhibited mCherry2 fluorescence.

Rat aortic SMC transfected with plasmids that encode PKGIγ exhibited increased SMC contractile protein expression in comparison with those exposed to the PKGIγ·ΔNLS-encoding or control vectors. As shown in Fig. 9B and C, SMC expressing PKGIγ but not PKGIγ-ΔNLS had increased numbers of cells exhibiting a higher mean fluorescence signal associated with calponin and MHC expression. Together these data indicate that PKGIγ regulates SMC differentiation through direct nuclear mechanisms.

4. Discussion

PKGI has a pivotal role in regulating how cGMP controls vascular SMC phenotype. Previous investigations demonstrated that PKGI increases the differentiation of SMC [1,23,25,26,51]. These studies led

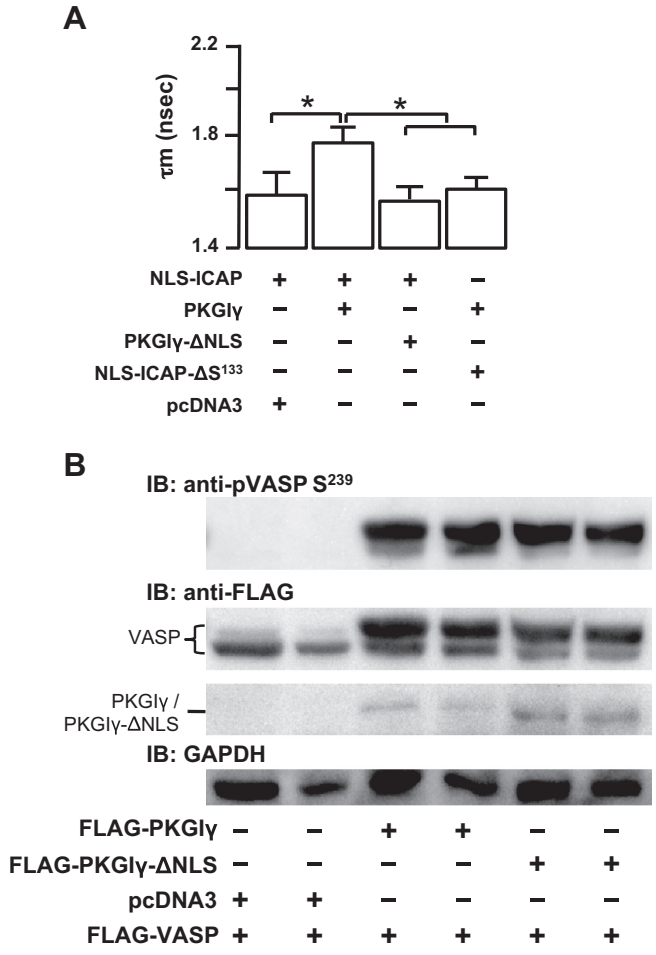

Fig. 5. Nuclear PKGIγ regulates phospho-CREB biosensor activation through a typical CREB KID PKA phosphorylation site. (A) BHK cells were transfected with plasmids encoding NLS-ICAP without and with a mutant serine corresponding to CREB S^{133} (NLS-ICAP-ΔS^{133}), the indicated PKGIγ transgenes, or pcDNA3, were fixed and then subjected to FLIM and the mean nuclear tm was obtained. Cells expressing PKGIγ exhibited increased NLS-ICAP CFP tm compared with those expressing PKGIγ-ΔNLS or transfected with pcDNA3. Importantly, PKGIγ expression did not change the CFP tm of NLS-ICAP-ΔS^{133} indicating that PKGIγ modulates NLS-ICAP CFP tm through targeting the S^{133} in CREB. $N = 15$ cells per group. (B) The PKGIγ-ΔNLS transgene exhibited typical cytoplasmic PKGI kinase activity in vivo. BHK cells transfected with plasmids that encode the indicated PKGIγ transgenes or pcDNA3 and FLAG-VASP, a cytosolic PKGI target, were lysed and the soluble proteins were resolved using SDS-PAGE, electro-blotted onto a charged membrane, and antigens were detected with the indicated antibodies, peroxidase labeled secondary antibodies, and enhanced chemiluminescence. FLAG-VASP exhibited phosphorylation and a typical increase in apparent molecular weight in lysates of cells expressing the PKGIγ transgenes but not transfected with the control plasmid.

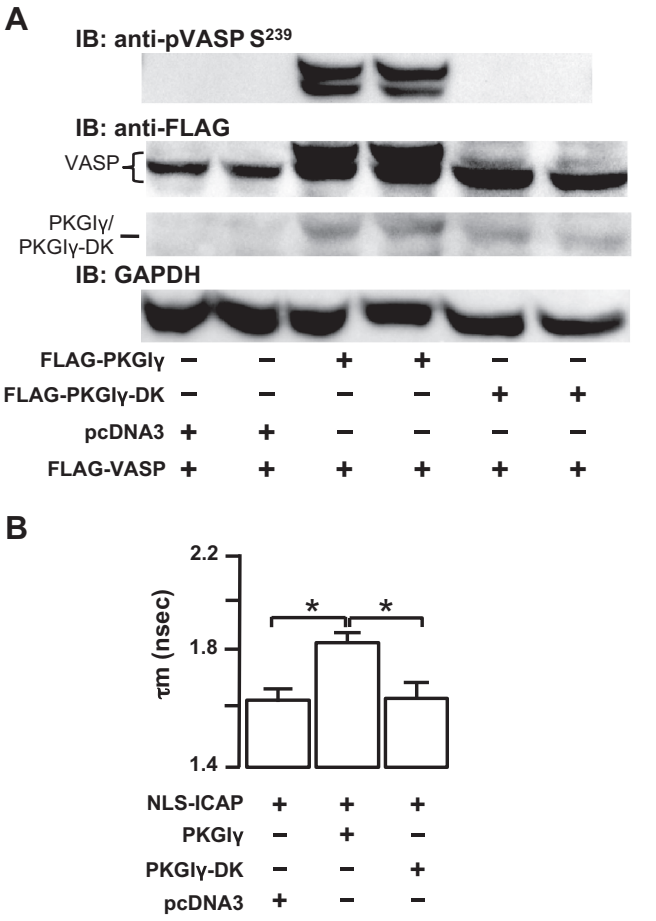

Fig. 6. PKGIγ kinase activity is required for nuclear phospho-CREB biosensor activation. (A) PKGIγ-DK lacks PKGI kinase activity. BHK cells were transfected with plasmids encoding NLS-ICAP, PKGIγ, or PKGIγ harboring a mutation previously shown to inhibit PKGIβ activity (PKGIγ-DK), or pcDNA3, as indicated, and FLAG-VASP were lysed and the soluble proteins were resolved using SDS-PAGE, electro-blotted onto a charged membrane, and antigens were detected with the indicated antibodies, peroxidase labeled secondary antibodies, and enhanced chemiluminescence. The lysates of cells transfected with the plasmid that encodes PKGIγ-DK did not exhibit FLAG-VASP phosphorylation or the typical shift of FLAG-VASP migration in SDS-PAGE associated with this post-translational modification. (B) BHK cells were transfected with plasmids encoding NLS-ICAP, the indicated PKGIγ transgenes, or pcDNA3, were fixed and then subjected to FLIM. The PKGIγ-DK expressing BHK cells did not exhibit changes in the nuclear CFP tm consistent with NLS-ICAP phosphorylation and CREB activation. $N = 15$ cells per group.

to the investigation of whether nuclear PKGI localization has a role in regulating the expression of SMC genes. Investigations identified a cryptic, cGMP-regulated NLS residing in the catalytic domain of PKGIβ that is required for PKGI nuclear compartmentation. Gudi et al. detected a single cluster of basic amino acids in PKGIβ that regulated the appearance of nuclear PKGI immunofluorescence and function, as detected by *fos* promoter activation [20]. This PKGIβ NLS amino acid sequence was thought to have a similar structure as one distinguished in interleukin-1α [20,52]. Although the general structure of NLSs is variable, we note that the putative PKGIβ NLS follows the consensus sequence of (K/R)X(K/R), which is thought to be typical of monopartite NLSs [53]. Moreover, this PKGIβ NLS resides within the Mg^{2+}/ATP binding region of the small lobe of the catalytic domain, which is likely to have access to the extramolecular environment and the adaptor proteins that are required to guide nuclear pore-dependent protein transport. Gudi et al. showed that the nuclear PKGI translocation was ATP-dependent, supporting the role of energy-dependent, nuclear pore-regulated PKGI nucleoplasm transport. The PKGIβ NLS also appeared to be cryptic because cGMP stimulation appeared to be important in activating the nuclear PKGI localization and activity. While characterizing the NLS activity, they observed that switching the P1 lysine to a negatively charged amino acid in the putative NLS generated a mutant PKGIβ that was catalytically active although it no longer exhibited cGMP-stimulated nuclear localization or transactivation of a *c-fos* promoter. In addition, fusing the putative NLS with β-galactosidase was found to be sufficient to cause the nuclear localization of that enzyme. However, in studies by other investigators, PKGI has been observed not to localize to the nucleus of cells and the putative PKGIβ NLS was shown to incompletely regulate cGMP-dependent PKGI nuclear compartmentation. For example, Collins and Euler observed that mutations of P1 and P3 amino acids in the putative PKGIβ NLS did not completely block the cGMP-stimulated PKGI nuclear activity in HEK293 cells [28]. Therefore, the mechanisms regulating nuclear PKGI translocation and activity are incompletely understood.

The work presented here provides important refinements to the knowledge about the mechanisms that regulate nuclear cGMP

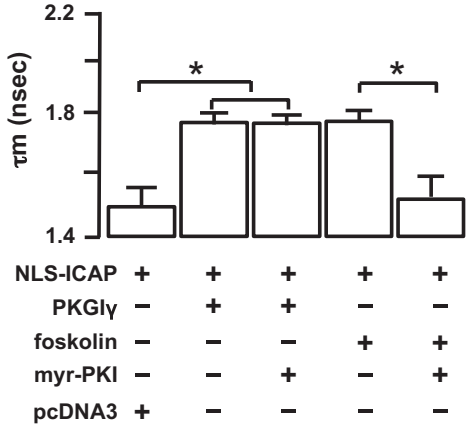

Fig. 7. PKGIγ regulates nuclear phospho-CREB biosensor activation in BHK cells through mechanisms that do not require PKA. The nuclear CFP tm values are shown of BHK cells transfected with plasmids expressing the indicated transgenes, or with pcDNA3, and treated with or without 40 μM forskolin and 10 μM myristoylated PKA inhibitor 14–22 amide (myr-PKI), as indicated. Myr-PKI did not inhibit the increase in NLS-ICAP CFP tm associated with PKGIγ although it did prevent the increase the activation of this phospho-CREB biosensor associated with forskolin treatment. $N = 15$ each group.

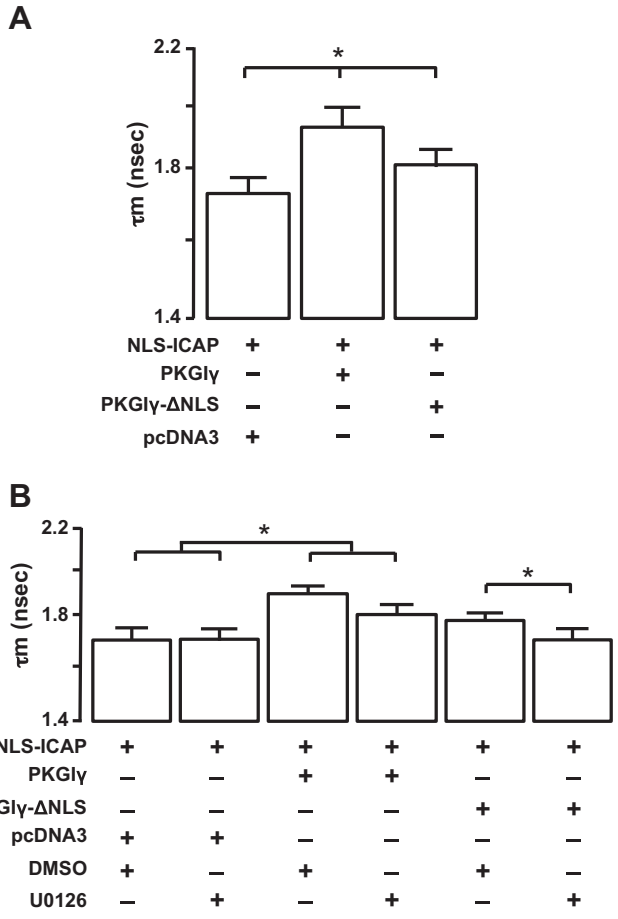

Fig. 8. Cytosolic PKGIγ regulates nuclear phospho-CREB biosensor activation in aortic SMC in part by modulating MAPK signaling. (A) Rat aortic SMC were transfected with plasmids encoding NLS-ICAP and either the indicated PKGIγ transgenes or pcDNA3. Subsequently, they were fixed and nuclear CFP tm was determined using FLIM. Both PKGIγ and PKGIγ-ΔNLS increased the activation of NLS-ICAP. (B) Rat aortic SMC were transfected as described above, treated with 10 μM U0126 or DMSO, the diluent, fixed, and then nuclear CFP tm was determined using FLIM. Although U0126 abolished the increase in the nuclear CFP tm observed in SMC expressing PKGIγ-ΔNLS, it only partially decreased the increased nuclear CREB activation observed in the cells expressing PKGIγ. Both A and B, $N = 15$ in each group.

signaling. Previously we showed that PKGI proteolysis plays a critical role in regulating nuclear PKGI localization [32]. In these studies, cGMP-treatment or PKGI overexpression in SMC or cell lines was observed to cause PKGI proteolysis and the generation of a COOH-terminal kinase fragment with constitutive activity. Moreover, we determined that although the NH_2-terminal LZ portion of cleaved PKGI is retained in the cytosol, the kinase fragment localizes to the nucleus. Using antibodies that detect the NH_2-terminal portion of the PKGI isoforms, we have not been able to detect full-length, uncleaved PKGI in the nucleoplasm. Although we observed that PKGI proteolysis was critical for nuclear PKGIγ localization and the regulation of gene expression by PKGIγ, the mechanisms controlling nuclear PKGIγ compartmentation were unknown.

PKGIγ is ~60 kDa and too large to passively diffuse into the nucleus. This is supported by our observation that PKGIγ with a mutation in the NLS was not immunolocalized to the nucleus and did not activate NLS-ICAP, unless mediated through cytosolic MAPK signaling. Moreover, the role of the NLS in PKGIγ nuclear transport is supported by studies of the compartmentation of synthetic PKGI catalytic domain fragments. For example, although Gudi et al. showed that whereas the putative NLS was not required for regulation of the nuclear compartmentation of a ~37 kDa fragment PKGIβ [20], it did control the nuclear localization and transactivation of gene expression by a 65 kDa fragment that contained more NH_2-terminal amino acids. Browning and colleagues showed that a ~63 kDa PKGI kinase fragment that was fused with GFP and contained the putative NLS, localized to the nucleus of cells [29]. Moreover, other investigators showed that COOH-terminal fragments of PKGI had important activities in regulating vascular SMC phenotype in cultured cells [23,54,55] and in injured systemic vessels [54]. However, in these studies, the role of nuclear localization in mediating these effects of the PKGI fragments in SMC was not investigated.

To further detail how the NLS characterized in this report influences PKGI nuclear localization, we examined whether importin α plays a part in regulating PKGIγ nuclear compartmentation. For these studies, we utilized a recently identified specific inhibitor of importin α and β-dependent protein localization. During the use of an AlphaScreen protein-protein binding assay designed to detect small molecules that disrupt viral protein nuclear import, ivermectin was identified as a potential inhibitor of importin α and β interaction [56]. Subsequently, this compound was determined to be a specific inhibitor of importin α and β-dependent nuclear localization using a variety of reference proteins [42]. Of interest, ivermectin did not inhibit the nuclear translocation of proteins that alone require importin β1 (e.g. parathyroid hormone-related protein [57]) or importin 13 (such as the SUMO-conjugating enzyme, UBC9 [58]) [42]. Our observation that ivermectin inhibits nuclear PKGIγ localization to similar levels observed for PKGIγ·ΔNLS indicate that importin α and β regulate PKGIγ nuclear compartmentation. The inhibition of GFP-NLS nuclear compartmentation by ivermectin was expected because the SV40 large T-antigen NLS encoded in this transgene has been shown to require importin α and β for nuclear localization regulation [59]. Moreover, Wagstaff showed that ivermectin inhibited the nuclear compartmentation of another fluorescent protein-SV40 large T-antigen fusion protein [42]. Together these results determine for the first time mechanisms that regulate PKGIγ nuclear localization in cells.

Previous studies have shown that PKGI activates gene expression. For example, PKGI proteolysis and nuclear PKGI compartmentation were observed to correlate with transactivation of phospho-CREB-dependent gene expression [20,32]. However, it is possible that this CREB-dependent gene regulation was modulated by activation of CREB in the cytosol and the nuclear translocation of phospho-CREB. For example, phospho-CREB has been detected in the cytosol of cells and other kinases have been observed to stimulate the nuclear localization of cytosolic phospho-CREB [44,45]. Therefore, to determine the role of the NLS characterized above in partitioning nuclear PKGIγ function, we employed a nuclear phospho-CREB based biosensor and mapped

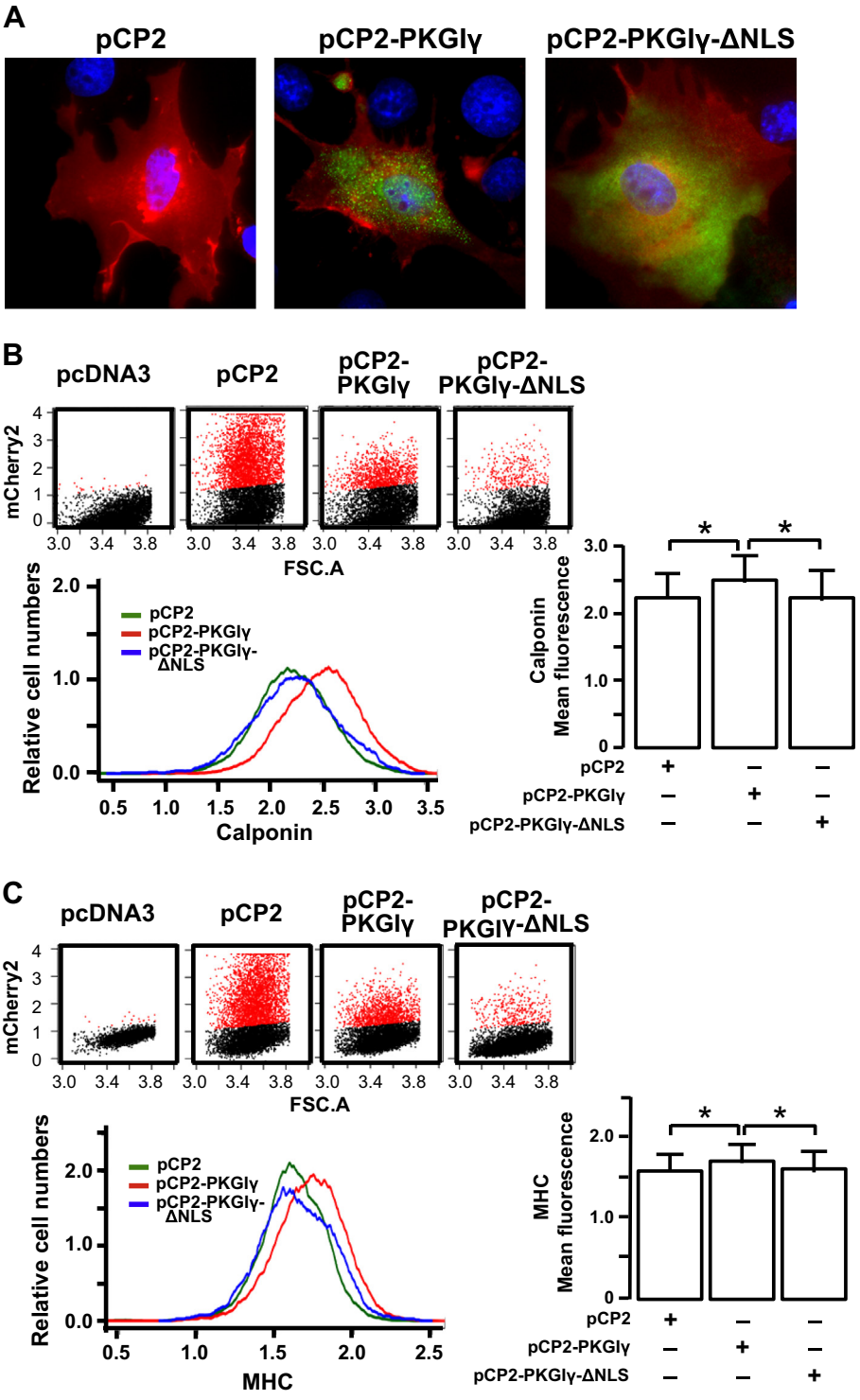

Fig. 9. PKGIγ but not PKGIγ-ΔNLS increases SMC differentiation marker expression levels in SMC. (A) Rat aortic SMC were transfected with bicistronic plasmids encoding mCherry2 in the second open reading frame (ORF), without (pCP2) or with FLAG-tagged PKGIγ transgenes encoded, as indicated, in the first ORF. Subsequently, the cells were fixed, permeabilized, and exposed to anti-FLAG and Alexa 488 anti-mouse IgG antibodies and subjected to epifluorescence microscopy. In these merged images of representative cells, the red, green, and blue colors represent mCherry2, anti-FLAG reactivity, and DAPI fluorescence signals, respectively. SMC transfected with the FLAG-PKGIγ, FLAG-PKGIγ-ΔNLS, and mCherry2-encoding plasmids exhibited anti-FLAG immunoreactivity and mCherry2 fluorescence indicating that mCherry2 expression effectively marks the transfected cells. (B and C) SMC were transfected with the plasmids noted above or pcDNA3. Subsequently they were dissociated from the plates, fixed, permeabilized, exposed to Alexa 488-labeled antibodies detecting calponin or MHC, and analyzed using flow cytometry. Following gating to include cells exhibiting mCherry2 fluorescence, here represented by the red data points in the scatter gram, it was determined that cells transfected with the plasmid encoding PKGIγ but not PKGIγ-ΔNLS exhibited increased expression of the SMC differentiation markers. The histogram shows the distribution of cells exhibiting the calponin and MHC fluorescence signal levels in the mCherry2-expressing SMC; the bar graph represents the mean fluorescence values related to the immunoreactivity of these SMC protein markers in the cells. A typical result of three independent experiments is shown.

its activation by PKGIγ in the nuclear compartment using FLIM. Friedrich et al. used phospho-specific antibodies and immunoblotting to show that PKA and CAM kinase phosphorylate this sensor and FRET methods to demonstrate that the biosensor is modulated within the nucleus of cells. Moreover, in the FLIM studies detailed here we observed that this sensor detects selective nuclear CREB activation, as we did not observe appreciable cytosolic NLS-ICAP CFP tm prolongations in cells expressing PKGIγ or PKGIγ-ΔNLS despite showing that the phosphorylation of a cytoplasmic PKGI target, FLAG-VASP. Moreover, using mutant NLS-ICAP and PKGIγ and PKA inhibitors, we confirmed that PKGIγ phosphorylated a typical PKA/PKGI motif, and did not modulate NLS-ICAP through cross-activation of PKA signaling. These data indicate that PKGIγ exhibits direct nuclear function, which is regulated through its nuclear compartmentation.

We found it interesting to note that, in contrast with the results observed in BHK cells, cytosolic PKGIγ activity regulated CREB activation in aortic SMC. These observations suggested that PKGIγ stimulates a cytosolic CREB-regulating signaling pathway that is not present in BHK cells. Previous investigators observed that PKGI activates MAPK signaling in aortic SMC [30]. Because this pathway stimulates CREB-signaling, we tested whether PKGIγ might regulate the phospho-CREB biosensor through cytoplasmic as well as nuclear mechanisms. Our observation of NLS-ICAP activation by PKGIγ-ΔNLS as well as PKGIγ in rat aortic SMC suggested this possibility. It is interesting that the lack of phospho-CREB sensor activation by PKGIγ-ΔNLS in BHK cells is consistent with the observations by others that PKGIβ does not stimulate MAPK signaling in these cells. This suggests that either the effector molecules might not be expressed or that PKGI might not share a similar cytosolic compartment with MAPK signaling components in these cells. Moreover, the inhibition of the NLS-ICAP activation by PKGIγ-ΔNLS by U0126 supports the potential role of MEK signaling in cytosolic PKGIγ activity. Nevertheless, the persistence of NLS-ICAP modulation in PKGIγ expressing U0126-treated cells supports a direct stimulation of CREB by nuclear PKGIγ in these cells.

Several studies indicate that PKGI regulates SMC differentiation. For example, PKGI expression reduction via cell passaging or RNAi, PKGI inhibition using membrane-permeable inhibitory peptides, and PKGI rescue by over-expression has been observed to modulate the mRNA and protein levels of contractile proteins in vascular SMC [1,25,51,60]. Moreover, over-expression of a COOH-terminal PKGI fragment that was engineered to have constitutive phosphokinase activity was observed to increase SMC contractile protein expression [23] and to decrease glucose- and serum-stimulated SMC proliferation in culture [54,55]. However, although PKGI has been determined to regulate nuclear signaling systems [20,22], it was unknown whether PKGI regulates SMC differentiation through nuclear or cytosolic mechanisms. We observed that PKGIγ but not PKGIγ·ΔNLS increased the protein expression of calponin and MHC in the SMC. These studies suggest that although PKGIγ can be observed to regulate cytosolic signaling systems, such as MAPK, the nuclear localization has an important role in controlling how it regulates SMC differentiation. These results lead us to speculate that mechanisms that inhibit the nuclear localization and activity of PKGIγ may play an important role in the pathogenesis of vascular diseases associated with SMC dedifferentiation.

5. Conclusion

We determined for the first time that an NLS residing in PKGIγ, an important constitutively active kinase fragment of PKGI in SMC, defines PKGI's role in regulating nuclear signaling and SMC phenotype determination. These findings are significant because they demonstrate that although PKGI can regulate nuclear signaling through cytoplasmic as well as nuclear pathways in SMC, it is the nuclear compartmentation of PKGIγ itself that plays a role in regulating SMC phenotype. Moreover, investigations detailed here promote the utility of using a nucleus-localizing CREB KID-based biosensor and FLIM in detailing nuclear PKGI function and the use of bicistronic plasmids with a fluorescent protein marker to examine the effects of gene expression on cell function in transfected SMC.

Acknowledgements

The US National Institutes of Health (R01HL096779) and the MGH Department of Anesthesia, Critical Care, and Pain Medicine supported this work. We are grateful to Drs. Michael Friedrich (Max Plank Institute of Neurobiology, Martinsried Germany) and Michael Uhler (Univ. of Michigan, Michigan USA) for providing plasmid reagents, to Dr. Gorin Martic for technical help in constructing the FLAG-PKGIγ construct, and to Drs. Angela Schmider, Roy Soberman, and the MGH Molecular Imaging Core Facility for providing technical support with the FLIM instrument.

References

[1] T.M. Lincoln, X. Wu, H. Sellak, N. Dey, C.S. Choi, Front. Biosci. 11 (2006) 356–367.
[2] S.H. Francis, J.L. Busch, J.D. Corbin, D. Sibley, Pharmacol. Rev. 62 (2010) 525–563.
[3] F. Hofmann, J.W. Wegener, Methods Mol. Biol. 1020 (2013) 17–50.
[4] P. Ruth, A. Pfeifer, S. Kamm, P. Klatt, W.R. Dostmann, F. Hofmann, J. Biol. Chem. 272 (1997) 10522–10528.
[5] R. Richie-Jannetta, S.H. Francis, J.D. Corbin, J. Biol. Chem. 278 (2003) 50070–50079.
[6] L.A. MacMillan-Crow, J.E. Murphy-Ullrich, T.M. Lincoln, Biochem. Biophys. Res. Commun. 201 (1994) 531–537.
[7] Y. Wang, M.R. El-Zaru, H.K. Surks, M.E. Mendelsohn, J. Biol. Chem. 279 (2004) 24420–24426.
[8] D.E. Casteel, T. Zhang, S. Zhuang, R.B. Pilz, Cell. Signal. 20 (2008) 1392–1399.
[9] R. Feil, N. Gappa, M. Rutz, J. Schlossmann, C.R. Rose, A. Konnerth, S. Brummer, S. Kuhbandner, F. Hofmann, Circ. Res. 90 (2002) 1080–1086.
[10] T.A. John, B.O. Ibe, J.U. Raj, Clin. Exp. Pharmacol. Physiol. 35 (2008) 148–158.
[11] M. Desch, K. Sigl, B. Hieke, K. Salb, F. Kees, D. Bernhard, A. Jochim, B. Spiessberger, K. Hocherl, R. Feil, S. Feil, R. Lukowski, J.W. Wegener, F. Hofmann, J. Schlossmann, Cardiovasc. Res. 86 (2010) 496–505.
[12] T.L. Cornwell, K.B. Pryzwansky, T.A. Wyatt, T.M. Lincoln, Mol. Pharmacol. 40 (1991) 923–931.
[13] W.G. Heil, W. Landgraf, F. Hofmann, Eur. J. Biochem. 168 (1987) 117–121.
[14] S. Orstavik, V. Natarajan, K. Tasken, T. Jahnsen, M. Sandberg, Genomics 42 (1997) 311–318.
[15] N.C. Browner, H. Sellak, T.M. Lincoln, Am. J. Physiol. Cell Physiol. 287 (2004) C88–C96.
[16] P.R. Bachiller, H. Nakanishi, J.D. Roberts Jr., Am. J. Physiol. Lung Cell. Mol. Physiol. 298 (2010) L324–L334.
[17] H. Sellak, C.S. Choi, N.B. Dey, T.M. Lincoln, Cardiovasc. Res. 97 (2013) 200–207.
[18] T.M. Lincoln, N. Dey, H. Sellak, J. Appl. Physiol. Respir. Environ. Exerc. Physiol. 91 (2001) 1421–1430.
[19] K.B. Pryzwansky, S. Kidao, T.A. Wyatt, W. Reed, T.M. Lincoln, J. Leukoc. Biol. 57 (1995) 670–678.
[20] T. Gudi, S.M. Lohmann, R.B. Pilz, Mol. Cell. Biol. 17 (1997) 5244–5254.
[21] T. Gudi, I. Huvar, M. Meinecke, S.M. Lohmann, G.R. Boss, R.B. Pilz, J. Biol. Chem. 271 (1996) 4597–4600.
[22] T. Gudi, D.E. Casteel, C. Vinson, G.R. Boss, R.B. Pilz, Oncogene 19 (2000) 6324–6333.
[23] N.J. Boerth, N.B. Dey, T.L. Cornwell, T.M. Lincoln, J. Vasc. Res. 34 (1997) 245–259.
[24] T. Zhang, S. Zhuang, D.E. Casteel, D.J. Looney, G.R. Boss, R.B. Pilz, J. Biol. Chem. 282 (2007) 33367–33380.
[25] W. Zhou, C. Dasgupta, S. Negash, J.U. Raj, Am. J. Physiol. Lung Cell. Mol. Physiol. 292 (2007) L1459–L1466.
[26] J.D. Chiche, S.M. Schlutsmeyer, D.B. Bloch, S.M. de la Monte, J.D. Roberts Jr., G. Filippov, S.P. Janssens, A. Rosenzweig, K.D. Bloch, J. Biol. Chem. 273 (1998) 34263–34271.
[27] N.C. Joyce, P. DeCamilli, J. Boyles, Microvasc. Res. 28 (1984) 206–219.
[28] S.P. Collins, M.D. Uhler, J. Biol. Chem. 274 (1999) 8391–8404.
[29] D.D. Browning, M. Mc Shane, C. Marty, R.D. Ye, J. Biol. Chem. 276 (2001) 13039–13048.
[30] P. Komalavilas, P.K. Shah, H. Jo, T.M. Lincoln, J. Biol. Chem. 274 (1999) 34301–34309.
[31] R. Schwappacher, J. Weiske, E. Heining, V. Ezerski, B. Marom, Y.I. Henis, O. Huber, P. Knaus, EMBO J. 28 (2009) 1537–1550.
[32] T. Sugiura, H. Nakanishi, J.D. Roberts Jr., Circ. Res. 103 (2008) 53–60.
[33] J.J. Kim, D.E. Casteel, G. Huang, T.H. Kwon, R.K. Ren, P. Zwart, J.J. Headd, N.G. Brown, D.C. Chow, T. Palzkill, C. Kim, PLoS ONE 6 (2011) e18413.
[34] S. Kato, R. Zhang, J.D. Roberts Jr., Am. J. Physiol. Lung Cell. Mol. Physiol. 305 (2013) L130–L140.
[35] M.W. Friedrich, G. Aramuni, M. Mank, J.A. Mackinnon, O. Griesbeck, J. Biol. Chem. 285 (2010) 23285–23295.
[36] R. Feil, J. Kellermann, F. Hofmann, Biochemistry 34 (1995) 13152–13158.
[37] B.W. Kimes, B.L. Brandt, Exp. Cell Res. 98 (1976) 367–381.
[38] D.J. Klinke II, K.M. Brundage, Cytometry A 75 (2009) 699–706.
[39] R Core Team, R Foundation for Statistical Computing, 2014. Vienna, Austria, URL http://www.R-project.org.

[40] D.S. Goldfarb, A.H. Corbett, D.A. Mason, M.T. Harreman, S.A. Adam, Trends Cell Biol. 14 (2004) 505–514.
[41] A. Harel, D.J. Forbes, Mol. Cell 16 (2004) 319–330.
[42] K.M. Wagstaff, H. Sivakumaran, S.M. Heaton, D. Harrich, D.A. Jans, Biochem. J. 443 (2012) 851–856.
[43] R.B. Pilz, K.E. Broderick, Front. Biosci. 10 (2005) 1239–1268.
[44] Y.M. Sue, C.P. Chung, H. Lin, Y. Chou, C.Y. Jen, H.F. Li, C.C. Chang, S.H. Juan, Am. J. Physiol. Cell Physiol. 297 (2009) C321–C329.
[45] W.J. Chen, Y.H. Chen, K.H. Lin, C.H. Ting, Y.H. Yeh, Arterioscler. Thromb. Vasc. Biol. 31 (2011) 2106–2113.
[46] W. Becker, J. Microsc. 247 (2012) 119–136.
[47] H.W. Ai, J.N. Henderson, S.J. Remington, R.E. Campbell, Biochem. J. 400 (2006) 531–540.
[48] M. Johannessen, U. Moens, Front. Biosci. 12 (2007) 1814–1832.
[49] G.A. Gonzalez, P. Menzel, J. Leonard, W.H. Fischer, M.R. Montminy, Mol. Cell. Biol. 11 (1991) 1306–1312.
[50] P.T. Winnard Jr., J.B. Kluth, Y. Kato, D. Artemov, V. Raman, Cancer Biol. Ther. 6 (2007) 1889–1899.
[51] N.B. Dey, K.F. Foley, T.M. Lincoln, W.R. Dostmann, J. Cardiovasc. Pharmacol. 45 (2005) 404–413.
[52] J.A. Maier, M. Statuto, G. Ragnotti, Mol. Cell. Biol. 14 (1994) 1845–1851.
[53] A. Lange, R.E. Mills, C.J. Lange, M. Stewart, S.E. Devine, A.H. Corbett, J. Biol. Chem. 282 (2007) 5101–5105.
[54] P. Sinnaeve, J.D. Chiche, H. Gillijns, N. Van Pelt, D. Wirthlin, F. Van De Werf, D. Collen, K.D. Bloch, S. Janssens, Circulation 105 (2002) 2911–2916.
[55] S. Wang, Y. Li, Am. J. Physiol. Heart Circ. Physiol. 297 (2009) H2075–H2083.
[56] K.M. Wagstaff, D.A. Jans, Anal. Biochem. 348 (2006) 49–56.
[57] M.H. Lam, W. Hu, C.Y. Xiao, M.T. Gillespie, D.A. Jans, Biochem. Biophys. Res. Commun. 282 (2001) 629–634.
[58] J.M. Mingot, S. Kostka, R. Kraft, E. Hartmann, D. Gorlich, EMBO J. 20 (2001) 3685–3694.
[59] C.Y. Xiao, S. Hubner, D.A. Jans, J. Biol. Chem. 272 (1997) 22191–22198.
[60] P. Li, D. Wang, J. Lucas, S. Oparil, D. Xing, X. Cao, L. Novak, M.B. Renfrow, Y.F. Chen, Circ. Res. 102 (2008) 185–192.